Behavior of the H atom velocity distribution function within the shock wave of a hydrogen plasma jet

S. Mazouffre, P. Vankan, R. Engeln, and D. C. Schram
Department of Applied Physics, Eindhoven University of Technology, P.O. Box 513, 5600 MB Eindhoven, The Netherlands
(Received 19 March 2001; revised manuscript received 9 July 2001; published 20 November 2001)

The evolution of the ground-state hydrogen atom velocity distribution function throughout the stationary shock wave of a supersonic hydrogen plasma jet ($3<$Mach number<4) is studied using laser-induced fluorescence spectroscopy. The H atom velocity distribution function may be decomposed into two Maxwellian distributions. The fast component of the distribution corresponds to the unhampered supersonic conditions. The slow component corresponds to the conditions in the shock region, i.e., within the shock front, the mean velocity and the temperature of this atom group vary. Across the shock wave, the H atom population is gradually transferred from the fast to the slow component by means of collisions. The development of the mean axial velocity is modeled using the Mott-Smith approach. Departure from the theoretical shock profile is interpreted in terms of the nonconservation of both the H atom forward flux and momentum across the shock wave.

DOI: 10.1103/PhysRevE.64.066405 PACS number(s): 52.35.Tc, 52.25.Fi, 47.40.Nm

I. INTRODUCTION

The study of physical systems under nonequilibrium conditions has been the subject of numerous researches for a long period of time. An example of a system characterized by a departure from thermodynamic equilibrium is the interior of a shock wave [1]. Across a shock wave, a flowing medium exhibits a rapid change in its macroscopic properties, i.e., density, velocity, and temperature, over a short distance (merely a few mean free paths). Shock waves are nowadays relatively easy to produce and to control using several kinds of experimental facilities such as wind tunnels, shock tubes, and free jets. Moreover, laboratory shock waves offer the possibility to cover a vast ensemble of physical conditions: a broad range of Mach numbers (M) is accessible, the flow regime may be varied from continuum to rarefied, the shock wave may be created in an atomic gas, a molecular gas or a plasma, to only name a few.

As recently pointed out by Ramos *et al.* [2], scientists are confronted with a paradox. Although the general properties of a shock wave are at present well established, there still exist numerous issues concerning the evolution of the distribution function within such a disturbed region. This peculiar situation is a direct consequence of the relative lack of detailed experimental studies in comparison with the large amount of theoretical works (see, for instance, [3–5] and references herein).

Most of experimental investigations of a gas (plasma) shock wave are devoted to the measurement of the development of macroscopic parameters. Several diagnostic techniques have been employed: electron-beam absorption [6] and electron-beam-induced fluorescence [7], Rayleigh scattering [8], laser-Doppler technique [9] and Thomson scattering [10]. Despite the fact that those studies furnish a large amount of data to be compared with the prediction of different theories, i.e., hydrodynamic approach (Navier-Stokes equation) or kinetic theory (Boltzmann equation), they only provide indirect information concerning the distribution function. Up until now, only a few works have been directly devoted to the study of the distribution function across a shock wave. In the work of Ramos *et al.* [2] the rotational state distribution function of N_2 molecules is studied in a nitrogen-free jet by means of Raman scattering, and in the work of Pham-Van-Diep, Erwin and Muntz [11] the velocity distribution function in a helium jet is measured by means of electron-beam-induced fluorescence. Those works confirm the main conclusions of Mott-Smith [12] and Glansdorff [13] about a bimodal distribution function in a shock region, even though the discovery of a third component, related with the invasion of the jet, is reported.

In the present contribution, the behavior of the velocity distribution function (VDF) of ground-state hydrogen atoms is directly studied within the stationary shock wave of a weakly ionized expanding hydrogen plasma ($3<M<4$, depending on the background pressure) by means of two-photon absorption laser induced fluorescence (TALIF) spectroscopy. From the VDF, the local H atom density, mean velocity, and temperature are also deduced. The large Doppler broadening of H atoms, combined with the relatively high temperature of the plasma medium, allows us to obtain accurate data on the VDF. In this plasma environment, we are confronted with a very particular situation: neither the H atom forward flux nor the H atom momentum is conserved within the shock wave [14]. A recombination of H atoms at the vessel walls induces large density gradients between the core of the plasma jet and its surrounding, which in turn, force H to diffuse out of the jet [15]. This effect is very pronounced in the shock region where the mean free path is large. Because of recombination processes in the arc nozzle, the expanding plasma is mainly composed of H_2 molecules to which H atoms transfer most of their momentum. As a consequence, the Rankine-Hugoniot relations are not valid for the H atom fluid, not even at high-background pressure.

II. EXPERIMENTAL ARRANGEMENT AND PLASMA JET

In the experiment reported in this contribution, ground-state hydrogen atoms are spatially probed by using a two-

photon absorption laser-induced fluorescence (TALIF) technique [16–18]. Since the experimental method has been described elsewhere [18], only a short overview is presented here. A tunable 20 Hz Nd:YAG pumped dye laser delivers radiation around 615 nm. The output of the dye laser is frequency-tripled resulting in 2 mJ of tunable UV light around 205 nm. The UV laser beam is focused into a vacuum chamber parallel to the plasma expansion axis. Hydrogen atoms are excited with two 205 nm photons from the $1s^2\,S$ ground state to the $3d^2\,D$ and $3s^2\,S$ states. The excitation is monitored by detection of the resulting fluorescence yield on the Balmer-α line at 656 nm using a gated photomultiplier tube. An interference filter is used to isolate the H_α line from the plasma emission. A slitmask is used to define the detection volume which dimensions are much smaller than any gradient length. The dye-laser frequency is accurately calibrated by the simultaneous recording of the absorption spectrum of molecular iodine. A spectral scan over the two-photon transition provide a direct access to the local H atom velocity distribution function (VDF), which allows for discussion on the state of equilibrium of the plasma flow. From the measured line profile, the H density and mean velocity are obtained. In the case of a Maxwellian distribution a H atom temperature may also be defined. The influence of the laser line profile [full width at half maximum (FWHM) $\approx 0.18\,\mathrm{cm}^{-1}$ at 205 nm] on the shape of measured spectral profile is neglected. This is legitimate in view of the low mass of H atoms and the relative high-plasma temperature.

The experimental determination of the velocity distribution function of a particle group is based on the Doppler effect. The broadening of a spectral line results from the Dopppler shift of the optical transition induced by the spread in velocity within a group of particles. A particle moving with velocity v_z towards a probing light source absorbs a photon at a frequency ν given by

$$\nu = \nu_0\left(1 - \frac{v_z}{c}\right), \tag{1}$$

where ν_0 is the absorption frequency of the particle at rest, c is the speed of light in vacuum. If the Doppler effect is the main broadening mechanism, the measured absorption profile is essentially the distribution of the velocity component v_z. Indeed, one cannot directly probe the three-dimensional (3D) velocity distribution $F_{\mathbf{v}}$, i.e., the density in velocity space, only the one-dimensional (1D) distribution $f_v(v_z)$ of the velocity component in the direction z of propagation of the laser beam is measured. The 1D and 3D velocity distribution function are related by

$$f_v(v_z) = \int\int F_{\mathbf{v}}\,dv_x\,dv_y, \tag{2}$$

which corresponds to a projection in velocity space. The energy distribution function $f_E(E)$ follows from a transformation of velocity into translational energy via $E=(1/2)mv^2$.

The hydrogen plasma is created by a cascaded arc [19]. The arc channel is composed of four insulated plates and has a diameter of 4 mm. The operating standard conditions are: a 55 A direct current, a cathode-anode voltage of 150 V and a H_2 gas flow of 3.5 standard liters per minute. The stagnation pressure inside the arc is 0.14 bar. The thermal hydrogen plasma expands from a straight nozzle with a diameter of 4 mm into a low-background pressure (p_{back}) chamber. At the arc outlet, the plasma turns into almost a hot gas, most electrons being consumed in the nozzle (ionization degree $<1\%$). Furthermore, the generation of H_2 molecules by a surface-recombination of H atoms is favored inside the arc nozzle that leads to a relatively low-dissociation degree at the source exit. Thus, H atoms flow in an environment mostly composed of H_2 molecules [14].

The flow pattern of H atoms in supersonic plasma jets generated from H_2 and from an Ar-H_2 mixture has been recently investigated by studying the H atom density, temperature, and velocity development during the expansion process [14,15,20]. In this contribution, we focus on the study of the plasma shock region with two main objectives: to examine the evolution of the H atom VDF in this region and to understand the related shock wave characteristics.

III. NONGAUSSIAN VDF WITHIN THE STATIONARY SHOCK WAVE

The behavior of the ground-state H atom VDF is examined throughout the normal shock wave of the expanding hydrogen plasma. The system being in stationary state, the VDF only depends on spatial coordinates. The VDF is measured along the jet centerline, namely, the velocity distribution is observed parallel to a stream line. Therefore, only the axial component of the H atom velocity is determined. The departure from thermodynamic equilibrium is directly reflected in the shape of the velocity distribution function, which markedly deviates from the Gaussian form, i.e., the equilibrium form, within the shock wave, as we will see.

Eight H atom velocity distribution functions recorded at different locations in the shock wave region are shown in Fig. 1 for a background pressure of 20 Pa. The local VDF is obtained from the measured spectral profile using the Doppler shift relation [see Eq. (1)] to switch from frequency space to velocity space. At $p_{\mathrm{back}}=20\,\mathrm{Pa}$, the normal shock wave stretches from $z=10\,\mathrm{mm}$ to $z=50\,\mathrm{mm}$. The Mach number prior to the shock equals four. The end of the shock is defined as the position where $M=1$.

Ahead of and behind the shock wave, the VDF is Gaussian. The corresponding energy distribution function is therefore Maxwellian, meaning that the H atom flow is in thermodynamic equilibrium. Throughout the stationary shock wave, there is a clear departure from thermodynamic equilibrium, since the VDF becomes non-Gaussian, as can be seen in Fig. 1. However, the H atom VDF may be decomposed into two Gaussian VDF corresponding to the unhampered supersonic conditions and the conditions in the shock region. This so-called bimodal approximation of the distribution function is not arbitrary, but it arises directly from the definition of a shock wave that is a transition zone where a supersonic flow has to adapt to the ambient subsonic conditions. It was first

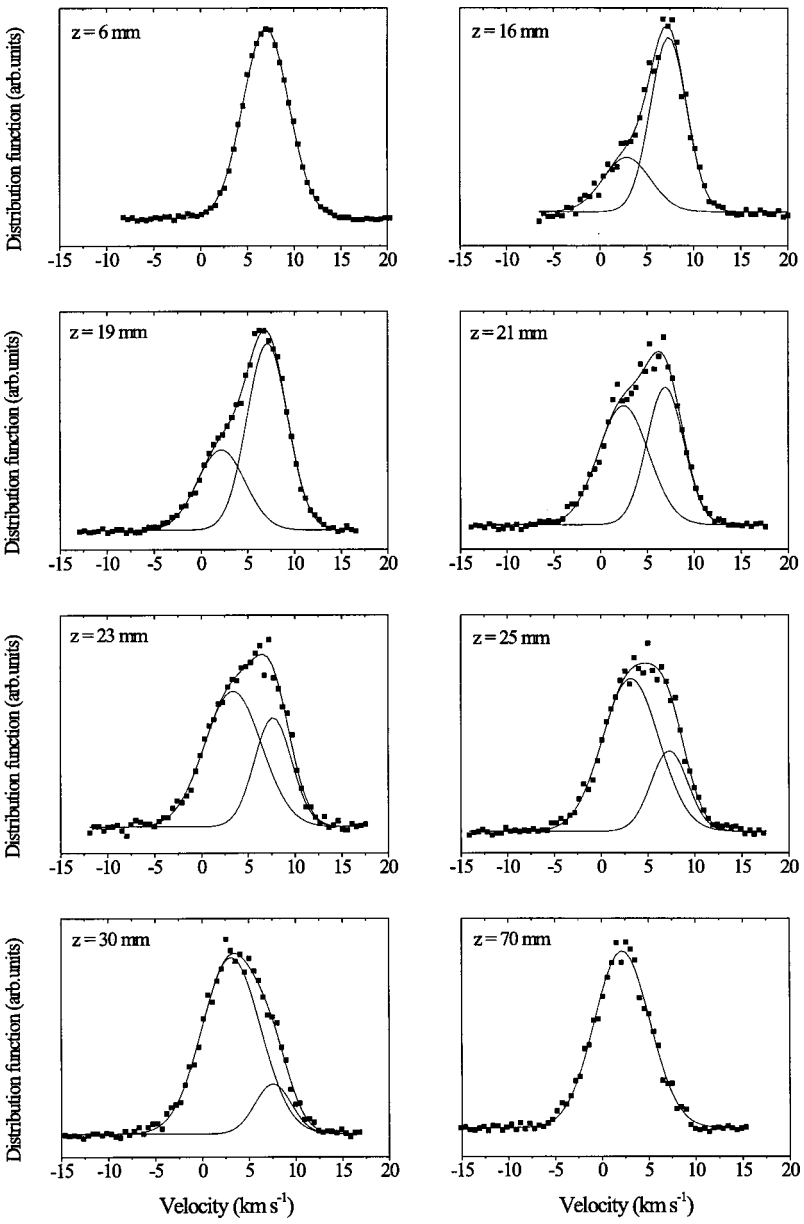

FIG. 1. Ground-state hydrogen atom velocity distribution function (VDF) measured at 20 Pa background pressure within the stationary shock wave of an expanding hydrogen plasma. In the shock region (10 to 50 mm), where departure from thermodynamic equilibrium is observed, the VDF consists of the sum of two Gaussian terms corresponding to the supersonic and the shock conditions.

proposed about half a century ago by Mott-Smith [12] and Glansdorff [13] in order to be able to solve the Boltzmann transport equation in a gas shock wave. A bimodal approximation for the H atom VDF across the shock wave is found to be also valid at a background pressure of 100 Pa, as shown in Fig. 2. At this pressure, the normal shock wave stretches from $z=6$ mm to $z=30$ mm, and $M=3$ prior to the shock.

Across the shock wave of the expanding plasma, the H atom population is gradually transferred from one group (the fast component with a VDF corresponding to the supersonic stream) to the other group (the slow component) by means of collisions with the background particles, i.e., H_2 molecules under our experimental conditions. This transfer of population, and the subsequent emergence of a bimodal VDF, is clearly visible in Figs. 1 and 2. In Fig. 3, we plotted the contents of the two Gaussian components as well as the total H atom density across the shock wave for a background pressure of 20 Pa. The emergence of the slow component and the disapearence of the fast component can easily be seen. Note that, due to plasma-wall interactions, the total H atom density does not increase across the shock wave [14,15,20]. At the end of the shock wave, all H atoms have changed from an initial supersonic Gaussian VDF to a final subsonic Gaussian VDF and the system returns to equilibrium. Note that all H atoms are thermalized (Gaussian VDF) before the end of the shock, i.e., they all have at least undergone one collision before the flow becomes subsonic. The fast component of the VDF contains only particles with a positive axial velocity whereas the slow component contains both particles with a positive and a negative axial velocity, and the dispersion in velocity (given by the width of the Gaussian VDF) is larger.

The H atom VDF within the shock region is well described by a bimodal approximation, as can be seen from the fit in Figs. 1 and 2. No evidence for the existence of a third component, the so-called scattered fraction, is experimen-

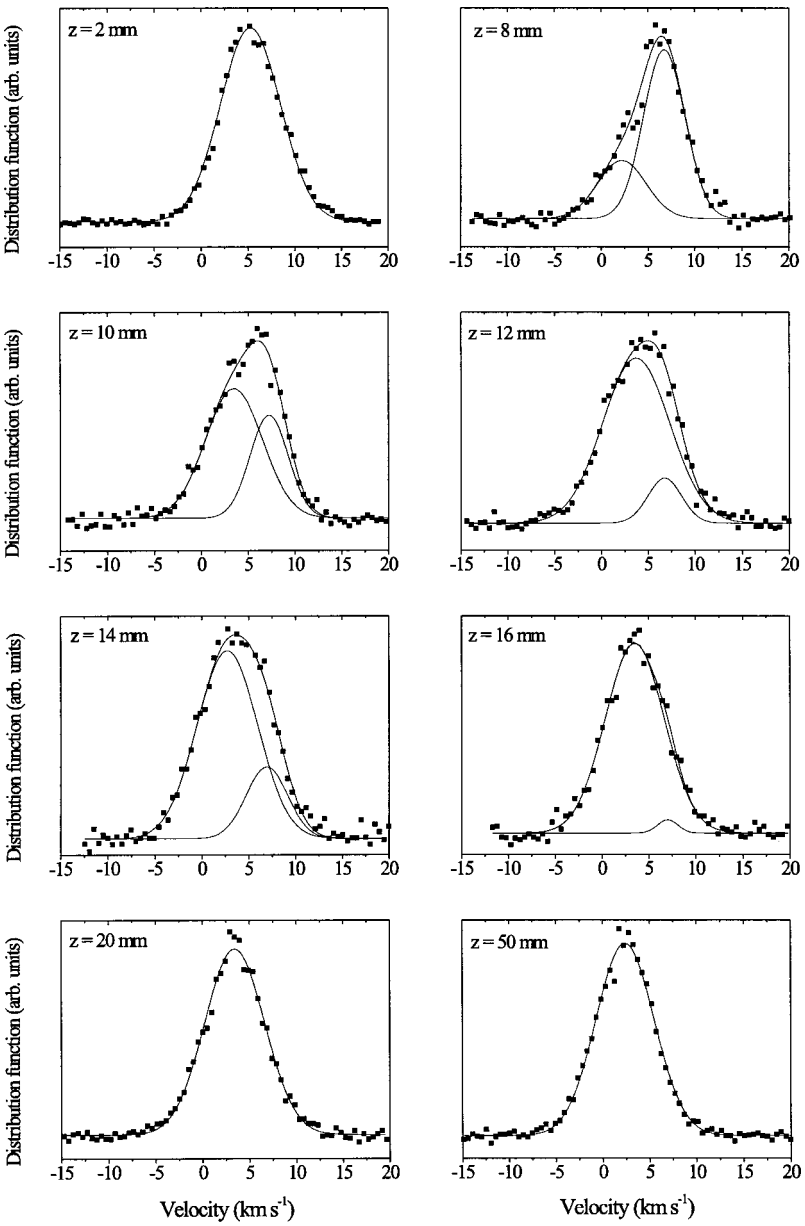

FIG. 2. Ground-state hydrogen atom velocity distribution function (VDF) measured at 100 Pa background pressure within the stationary shock wave of an expanding hydrogen plasma. In the shock region (6 to 30 mm), where departure from thermodynamic equilibrium is observed, the VDF consists of the sum of two Gaussian terms corresponding to the supersonic and the shock conditions. It can be seen that all H atoms are thermalized (Gaussian VDF) ahead of the end of the shock wave.

tally found, contrary to what is reported in previous studies [2,11,21]. In References [11] and [21], one-dimensional VDF measured in He and Ar shock waves are compared with predictions from Monte Carlo direct simulation (MCDS) method based on realistic interatomic potential. An excellent agreement is found between experimental data and data calculated using MCDS. In particular, the MCDS method is able to predict the existence of a third group of particles. In other words, in those gas shock waves, the Mott-Smith approach fails to represent the distribution function (Mott-Smith and MCDS predictions are compared in Ref. [11]).

In our case, the validity of a bimodal model may arise from the fact that, contrary to the Mott-Smith approach, the slow VDF does not correspond to the conditions downstream of the zone of silence but it corresponds to the conditions in the shock wave. In other words, as we will see in the next section, the mean velocity and the temperature of the slow Gaussian component vary through the shock region, and therefore this component accounts for mixing effects [11,21].

The scattered component may also originate from gas particles that penetrate the shock region from the jet boundary and from the Mach disk. This invasion may lead to the appearance of a third fraction since the initial VDF of these particles (as measured along a stream line) is neither the fast one nor the slow one. Under our experimental conditions, due to wall-association processes, H atoms are almost absent in the background gas. As a consequence, the shock wave is invaded mainly by H_2 molecules, and no H atom scattered distribution is formed. The appearance of a third fraction in the VDF would in that case merely be visible in the H_2 molecule VDF. Note that this effect should be more pro-

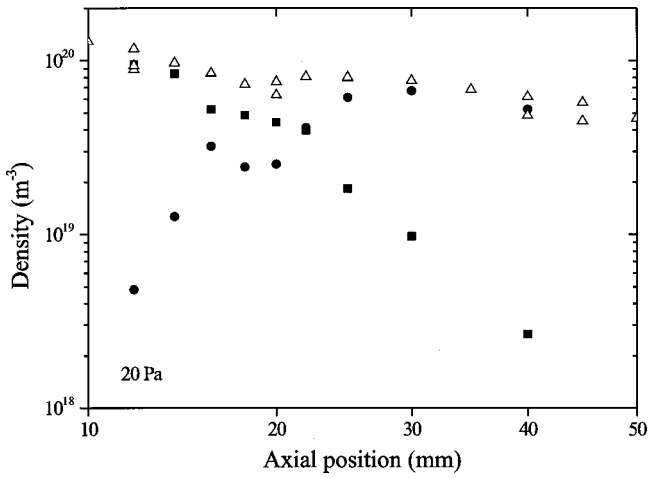

FIG. 3. On-axis profile of the total H atom density, i.e., the contents of the VDF, across the stationary shock wave at 20 Pa background pressure (open triangle). The population of the fats component (solid square) decreases to finally vanish whereas the population of the slow component (solid circle) increases. At the end of the shock wave, only subsonically flowing H atoms remain.

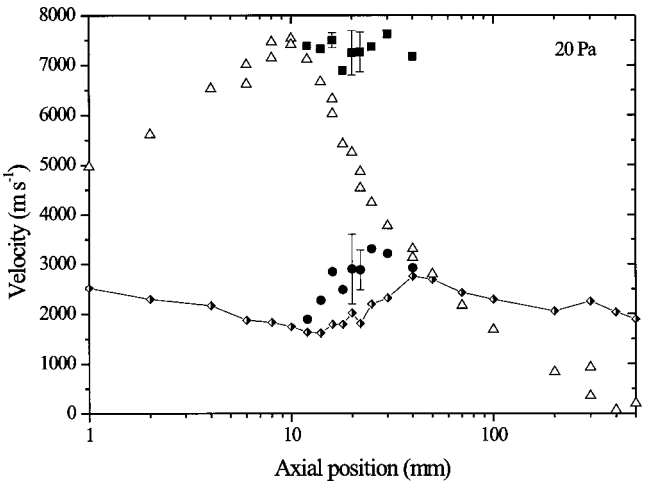

FIG. 4. Profile of the H atom axial velocity (open triangle) along the jet centerline at 20 Pa background pressure. Throughout the shock wave, the average H atom velocity is calculated from the first moment of the distribution function. The mean velocity of both the fast (solid square) and the slow (solid circle) component of the VDF are shown in the shock region. Also shown is the axial profile of the speed of sound (diamond) determined from the measured H atom parallel temperature.

nounced at low-background pressure where the invasion of the shock region by the background gas is favored [22,23].

IV. VELOCITY AND TEMPERATURE PROFILES ALONG THE JET AXIS

From the measured H atom velocity distribution function, a mean axial velocity as well as a parallel temperature, which represents the spread in velocity along a stream line, may be calculated for each Gaussian component. The velocity is determined from the Doppler shift of the peak. The temperature is determined from the Doppler broadening of the peak, which is the dominant broadening mechanism in our case, taking into account the bandwidth of the laser profile that is assumed to be gaussian.

Throughout the stationary shock wave the average H atom axial velocity is obtained from the first moment of the VDF. In this region, the H atom parallel temperature may not be strictly defined since the flowing medium is not in thermodynamic equilibrium. We attempt however to define an average local parallel temperature $\hat{T}_{\parallel}$ that may be seen as the temperature that would be given by a hypothetical thermometer plunged into the shock region (ignoring the perpendicular temperature). This average temperature is calculated by weighting the temperature of the two Gaussian components with their corresponding density

$$\hat{T}_{\parallel}=\frac{n_{\mathrm{fast}}T_{\parallel\mathrm{fast}}+n_{\mathrm{slow}}T_{\parallel\mathrm{slow}}}{n_{\mathrm{fast}}+n_{\mathrm{slow}}}, \tag{3}$$

where the subscript *fast* and *slow* refers to the fast component and the slow component of the distribution function, respectively.

Before analyzing the axial profile of the H atom velocity v and temperature T, it is of interest to briefly discuss the experimental uncertainty on these two macroscopic parameters. Three different sources of uncertainty may be identified. The first two are the approximate laser bandwidth, which introduces noise in the deconvolution step necessary to obtain T, and the inaccuracy in the position of the iodine peaks [18], which generates uncertainty in the calibration of the velocity axis. The error in v and T that results from these two sources is $\Delta v=\pm 200\,\mathrm{ms}^{-1}$ and $\Delta T=\pm 20\,\mathrm{K}$. Another important source of error (independent from the first two) is the fitting procedure used to determine the Gaussian distributions. Using different programs and methods, the uncertainty that arises from the fitting procedure, is estimated to be $\Delta v=\pm 150\,\mathrm{ms}^{-1}$ and $\Delta T=\pm 140\,\mathrm{K}$. Thus, the experimental statistical uncertainty is found to be $\pm 250\ \mathrm{ms}^{-1}$ and ± 140 K for the velocity and the temperature, respectively [24].

The H atom velocity profile along the plasma jet centerline is shown in Fig. 4 at $p_{\mathrm{back}}=20\,\mathrm{Pa}$ and in Fig. 5 at $p_{\mathrm{back}}=100\,\mathrm{Pa}$. On both graphs, the measured velocity is compared with the local speed of sound calculated from the measured H atom parallel temperature ($\hat{T}_{\parallel}$ across the shock wave) and using $m=2$ amu since the jet is mainly composed of H_2 molecules. The corresponding on-axis development of the H atom parallel temperature is shown in Fig. 6 at $p_{\mathrm{back}}=20\,\mathrm{Pa}$ and in Fig. 7 at $p_{\mathrm{back}}=100\,\mathrm{Pa}$. The general shape of both the velocity and the temperature profile in the course of the plasma expansion has already been explained in preceding articles [14,15]. In this contribution, we only focus on the shock region.

The fast component of the H atom VDF, i.e., the component that corresponds to the unhampered supersonic conditions, represents the fraction of hydrogen atoms that have not yet collided with the particles of the shock wave region, namely, H_2 molecules. This component thus exhibits the flow

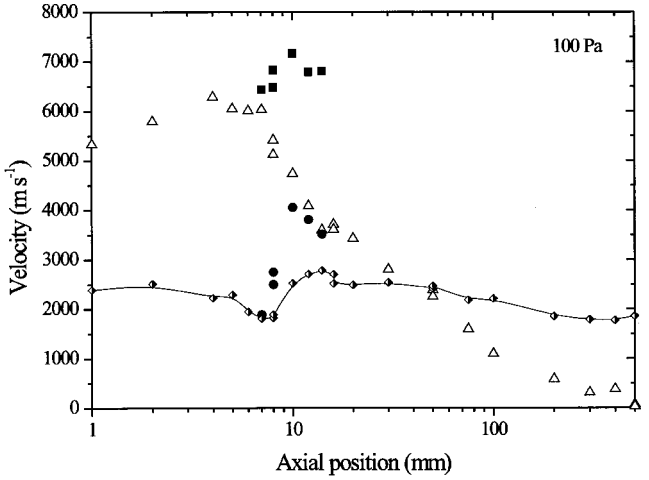

FIG. 5. Profile of the H atom axial velocity (open triangle) along the jet centerline at 100 Pa background pressure. Throughout the shock wave, the average H atom velocity is calculated from the first moment of the distribution function. The mean velocity of both the fast (solid square) and the slow (solid circle) component of the VDF are shown in the shock region. Also shown is the axial profile of the speed of sound (diamond) determined from the measured H atom parallel temperature.

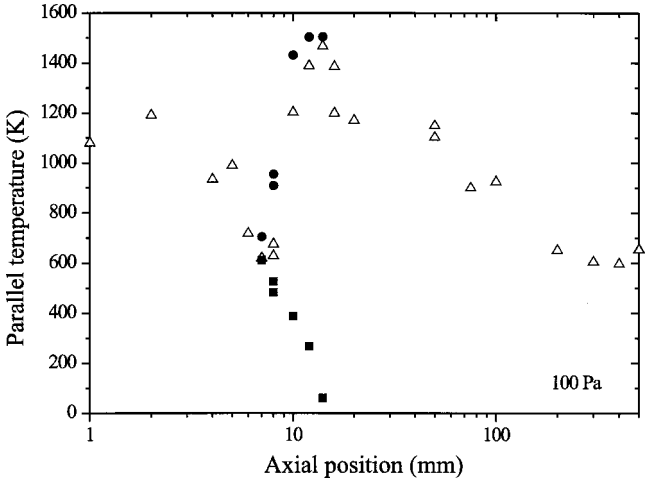

FIG. 7. On-axis profile of the H atom parallel temperature (open triangle) at a background pressure of 100 Pa. Throughout the shock wave, an average temperature is determined from the temperature of the two Gaussian components of the distribution function [see Eq. (3)]. The temperature of both the fast (solid square) and the slow (solid circle) component of the VDF are also shown in the shock region.

properties of a supersonic beam [25]. The mean H atom axial velocity of the fast component remains high. At 20 Pa background pressure, the velocity is frozen at about 7500 ms^{-1}, whereas at 100 Pa, the velocity still increases across the shock wave, meaning that H atoms may still convert part of the thermal energy they gained in the plasma source into kinetic energy. The corresponding parallel temperature decreases down to 300–200 K, meaning that the spread in velocity decreases. The fast component of the VDF is thus often referred to as the cold component.

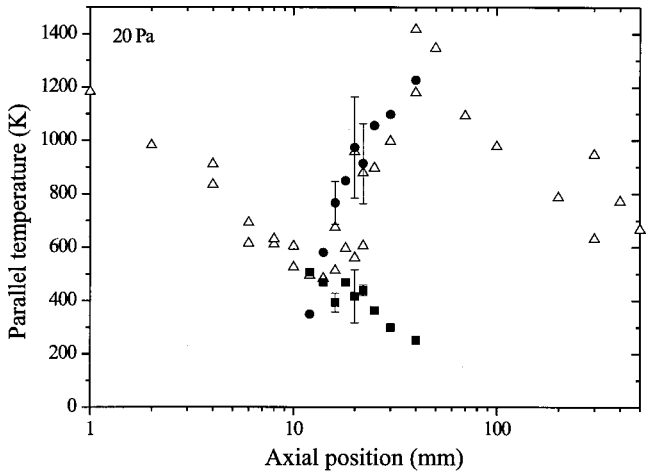

FIG. 6. On-axis profile of the H atom parallel temperature (open triangle) at a background pressure of 20 Pa. Throughout the shock wave, an average temperature is determined from the temperature of the two Gaussian components of the distribution function [see Eq. (3)]. The temperature of both the fast (solid square) and the slow (solid circle) component of the VDF are also shown in the shock region.

The slow component of VDF, i.e., the component that corresponds to the conditions in the shock wave, contains H atoms that have at least experienced one collision with the particles located in the shock region. The mean axial velocity is low at the beginning of the shock region, around 2000 ms^{-1}. It increases across the shock wave due to collisions slow H atoms undergo with supersonically flowing particles. The rise of the mean velocity of the VDF slow component is faster at the beginning of the shock region, as can be seen in Figs. 4 and 5. It arises from the fact that collisions of slow H atoms with fast H_2 molecules (the main collision partner) become quickly scarce because the population of the fast VDF component of H_2 drops also fast across the shock wave to finally disappear. The temperature of the slow component is relatively high. It increases because kinetic energy is converted into thermal motion in a collision involving a fast H atom. In other words, directed motion is transformed into random motion within a shock wave. The slow component of the VDF is also often called the warm component.

V. THEORETICAL VELOCITY PROFILE IN THE SHOCK REGION: MOTT-SMITH APPROACH

The H atom average velocity measured throughout the stationary shock wave along the plasma jet centerline may be compared with a theoretical model based on a bimodal approximation of the velocity distribution function. Across a shock front, the density profile as well as the corresponding velocity profile of the flowing fluid may be calculated as shown by Mott-Smith [12] and Glansdorff [13]. The centerline velocity is given by

$$v(\tilde{z}) = \frac{v_2(1+e^{4\tilde{z}/L})}{(v_2/v_1)+e^{4\tilde{z}/L}}, \tag{4}$$

where $\tilde{z}=z-z_0$, z_0 being the center of the shock wave (point of inflection), v_1 and v_2 are the velocity ahead of and behind the shock, respectively, and L is the shock thickness defined as

$$L=(v_1-v_2)\left.\frac{dz}{dv}\right|_{\max}, \tag{5}$$

according to the Prandtl formalism [26]. We found that $L=16.8$ and 9.7 mm at 20 and 100 Pa, respectively. The velocity may also be expressed as a function of the Mach number M ahead of the shock front and the adiabatic exponent γ using the Rankine-Hugoniot relations. In order to make the results independent of the conditions, one may define a normalized velocity in the following way:

$$\tilde{v}(\tilde{z})=\frac{v(\tilde{z})-v_2}{v_1-v_2}. \tag{6}$$

When the measured (normalized) velocity is to be compared with the theoretical (normalized) velocity given by Eq. 4 (Eq. 6) a scaling length S needs to be introduced to take into account the shift in position between the inflection point of the density curve and the velocity curve. The parameter S is given by

$$S=\frac{L}{4}\ln\frac{v_2}{v_1}. \tag{7}$$

For high Mach number ($M>2$), the bimodal method is known to describe properly the shock wave structure [6,7]. The comparison between experiments and calculations is shown in Fig. 8. As can be seen from the graph, the agreement is relatively good at the beginning of the shock wave even if the normalized velocity profile measured at 100 Pa deviates slightly from the predictions. However, in the final part of the shock region, a strong deviation is observed. This effect has already been reported in literature in the case of on-axis density profiles measured in neutral gas shock waves [2,6,7]. It arises from the fact that the model developed by Mott-Smith is a one-dimensional (1D) normal shock wave model that does not account for scattering effects. Such effects, related to the invasion of the supersonic jet by the background gas, occurs for a 2D shock wave when the flow enters the rarefied regime [22], i.e, when the Knudsen number Kn is large. It has indeed been observed that at high-background pressure, the agreement between experimental data and the Mott-Smith model is good and it deteriorates at low pressure. The Knudsen number ahead of a shock wave is the ratio of the mean free path for momentum exchange to the shock thickness. It reads

$$Kn=\frac{1}{n_{H_2}\sigma_{H-H_2}L}. \tag{8}$$

The temperature-dependent momentum exchange cross-section σ_{H-H_2} is taken from literature [27] and the H_2 density has been measured by means of coherent anti-Stokes Raman spectroscopy (CARS) [28]. Under our conditions, Kn$=0.7$ at 20 Pa and Kn$=0.2$ at 100 Pa ahead of the shock wave meaning that the latter is formed in a transition flow regime. Surprisingly, the H atom velocity profile measured at $p_{\text{back}}=20$ Pa and the one measured at $p_{\text{back}}=100$ Pa exhibit a similar behavior in the final part of the shock wave, as can be seen in Fig. 8, in contradiction with measurements reported in literature [2]. The two normalized velocity profiles deviate in approximately the same way from the theoretical calculation. In other words, there is no clear influence of the background pressure. This remarkable fact is a consequence of the nonconservation of both the H atom forward flux and the H atom momentum throughout the stationary shock wave of the plasma jet [14,15,20]. In that case, the Mott-Smith approach used to calculate the average velocity is not valid since it is based on the Rankine-Hugoniot relations. A theoretical calculation of the H atom velocity profile within the normal shock wave would therefore require a 2D model capable of accounting for a decoupling between the H atom fluid and the H_2 molecule fluid induced by H atom surface-recombination processes.

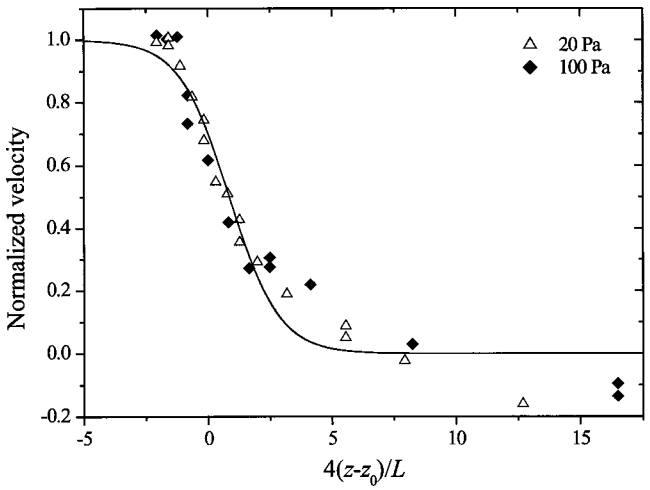

FIG. 8. Normalized H atom velocity [see Eq. (6)] profile within the stationary shock wave of an expanding hydrogen plasma at 20 Pa (open triangle) and at 100 Pa (solid diamond) background pressure. The parameter z_0 corresponds to the center of the shock wave and L is the shock thickness. The solid line represents the calculated normalized velocity profile under the assumption of a bimodal distribution function based on the theory developed by Mott-Smith [12] and Glansdorff [13].

VI. CONCLUSIONS

The specific ground-state hydrogen atom shock wave pattern formed in a weakly ionized hydrogen plasma jet may serve as a test case to validate predictions of kinetic models based on the Boltzmann equation used to study the behavior of the velocity distribution function and the fluid macroscopic properties within a shock wave. The two-photon absorption laser-induced fluorescence spectroscopy is well-

adapted to extract local information about ground-state atoms at a microscopic scale, both in a gas and in a plasma environment. Using this diagnostic tool, one may provide large datasets to support theoretical studies devoted to the shock wave properties. Such data are also of relevance in order to better understand the shock wave formation at low-background pressure and the related invasion of the shock region by the residual gas particles, which is of interest in various fields like astrophysics and plasma-assisted chemistry.

ACKNOWLEDGMENTS

The authors would like to acknowledge fruitful discussion with Professor M.C.M. van de Sanden. The authors greatly appreciate the skillful technical assistance of M.J.F. van de Sande, A.B.M. Hüsken, and H.M.M. de Jong. This work is part of the research program of the Netherlands Foundation for Fundamental Research on Matter (FOM). It is financially supported by the Dutch Organization for Scientific Research (NWO) as well as the Euratom Foundation.

[1] Y. B. Zel'dovich and Y. P. Raizer, *Physics of Shock Waves and High Temperature Hydrodynamic Phenomena* (Academic Press, New York, 1966), Vol. 1-2.
[2] A. Ramos, B. Maté, G. Tejeda, J. M. Fernández, and S. Montero, Phys. Rev. E **62**, 4940 (2000).
[3] F. J. Uribe, R. M. Velasco, L. S. García-Colín, and E. Díaz-Herrera, Phys. Rev. E **62**, 6648 (2000).
[4] S. Takata, K. Aoki, and C. Cergignani, Phys. Fluids **12**, 2116 (2000).
[5] C. Cercignani, A. Frezzotti, and P. Grosfils, Phys. Fluids **11**, 2757 (1999).
[6] H. Alsmeyer, J. Fluid Mech. **74**, 497 (1976).
[7] F. Robben and L. Talbot, Phys. Fluids **9**, 653 (1966).
[8] J. Panda and R. G. Seasholtz, Phys. Fluids **11**, 3761 (1999).
[9] P. L. Eggins and D. A. Jackson, J. Phys. D **7**, 1894 (1974).
[10] M. C. M. van de Sanden, R. van den Bercken, and D. C. Schram, Plasma Sources Sci. Technol. **3**, 511 (1994).
[11] G. Pham-Van-Diep, D. Erwin, and E. P. Muntz, Science **245**, 624 (1989).
[12] H. M. Mott-Smith, Phys. Rev. **82**, 885 (1951).
[13] P. Glansdorff, Phys. Fluids **5**, 371 (1962).
[14] S. Mazouffre, P. J. W. Vankan, R. Engeln, and D. C. Schram, Phys. Plasmas **8**, 3824 (2001).
[15] S. Mazouffre, M. G. H. Boogaarts, J. A. M. van der Mullen, and D. C. Schram, Phys. Rev. Lett. **84**, 2622 (2000).
[16] U. Czarnetzki, K. Miyazaki, T. Kajiwara, K. Muraoka, M. Maeda, and H. F. Döbele, J. Opt. Soc. Am. B **11**, 2155 (1994).
[17] H. W. P. van der Heijden, M. G. H. Boogaarts, S. Mazouffre, J. A. M. van der Mullen, and D. C. Schram, Phys. Rev. E **61**, 4402 (2000).
[18] S. Mazouffre, M. G. H. Boogaarts, R. Engeln, J. A. M. van der Mullen, and D. C. Schram, in Proceedings of Laser-Aided Plasma Diagnostics, Lake Tahoe, California, 1999, Vol. 9, p. 320.
[19] G. M. W. Kroesen, D. C. Schram, and J. C. M. de Haas, Plasma Chem. Plasma Process. **10**, 551 (1990).
[20] S. Mazouffre, R. Engeln, M. G. H. Boogaarts, J. A. M. van der Mullen, and D. C. Schram, in Proceedings of Thermal Plasma Processing, Strasbourg, France, 2000, Vol. 6, p. 83.
[21] D. A. Erwin, G. C. Pham-Van-Diep, and E. P. Muntz, Phys. Fluids A **3**, 697 (1991).
[22] E. P. Muntz, B. B. Hamel, and B. L. Maguire, AIAA J. **8**, 1651 (1970).
[23] R. Compargue, J. Chem. Phys. **52**, 1795 (1970).
[24] J. R. Taylor, *An Introduction to Error Analysis* (University Science Books, Oxford University, New York, 1982).
[25] *Atomic and Molecular Beam Methods*, edited by G. Scoles (Oxford University, New York, 1988).
[26] C. Muckenfuss, Phys. Fluids **3**, 320 (1960).
[27] A. Phelps, J. Phys. Chem. Ref. Data **19**, 653 (1996).
[28] R. F. G. Meulenbroeks, R. A. H. Engeln, J. A. M. van der Mullen, and D. C. Schram, Phys. Rev. E **53**, 5207 (1996).